

Notes

Structure of Shear-Induced Perforated Layer Phase in Styrene–Isoprene Diblock Copolymer Melts

Jong-Hyun Ahn and Wang-Cheol Zin*

Department of Materials Science & Engineering and Polymer Research Institute, Pohang University of Science and Technology, Pohang, Kyungbuk, 790-784, Korea

Received August 2, 1999

Revised Manuscript Received November 15, 1999

Diblock copolymers self-assemble into a variety of ordered microstructures due to the immiscibility between the two different blocks comprising the polymer molecule.¹ Its phase behaviors depend primarily on three factors: (i) the volume fraction of one monomer unit, f , (ii) the degree of polymerization, N , and (iii) the interaction parameter, χ . For symmetric copolymers with $f = 0.5$, the melt is ordered into a lamellar structure. As f is increased, a cylindrical phase and a spherical phase are commonly observed. Besides the classical phases, recent experiments have revealed the existence of new phases in a narrow range of f and χN between the lamellar and cylindrical phases.^{2–14} The additional phases are the gyroid (G) with $Ia\bar{3}d$ space group symmetry^{6–12} and hexagonally perforated layers (HPL).^{2,7–11} The structure of the G phase has been well characterized by small-angle neutron scattering (SANS) and transmission electron microscopy (TEM). Many theoretical studies have also found this phase to be stable.^{16–18} On the other hand, the structural nature of HPL phase has not been fully resolved. On the basis of small-angle scatterings and transmission electron microscopy studies, it is believed that the HPL structure consists of alternating minority and majority component layers in which hexagonally packed channels of majority component extend through the minority component. The stacking sequences of HPL channels can be modeled as both ABAB... and ABCABC... patterns, as illustrated in Figure 1. Förster et al. have proposed that the perforation of HPL is stacked in ABCABC... pattern for styrene–isoprene diblock copolymers with $0.61 < f_{PS} < 0.65$ through the interpretation of SANS data.⁸ However, the higher order scattering patterns have not been observed to prove clearly ABCABC... stackings. In more recent studies, Vigild et al. have observed long-range oriented HPL structures of ethylenepropylene–dimethylsiloxane diblock copolymer mixtures using the small-angle X-ray scattering (SAXS).¹⁴ Unlike the findings of Förster et al., Vigild et al. have reported that the HPL structure is composed of a combination of an ABCABC... and ABAB... arrangement, i.e., as a combination of a face-centered cubic and a hexagonally close-packed

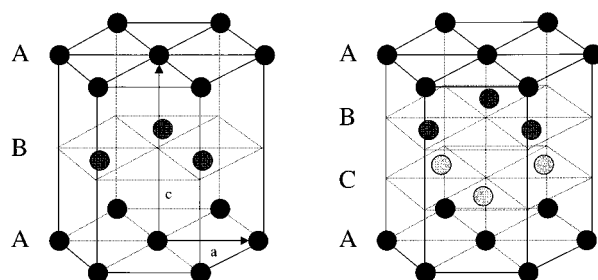


Figure 1. Hexagonal lattice models for (a) ABAB... and (b) ABCABC... stacking sequence. The letters c and a denote the parameters of lattice.

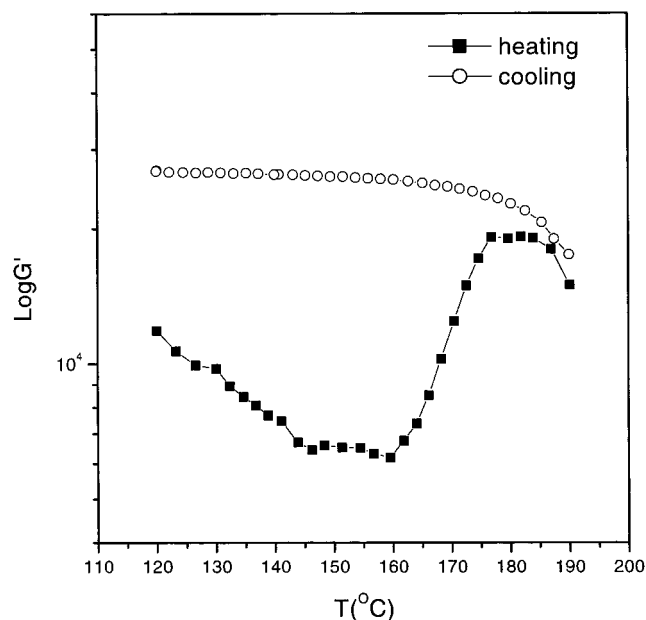


Figure 2. Temperature dependence of dynamic shear moduli for PSI67 at shearing conditions of $\omega = 0.1$ rad/s, $\gamma = 1\%$, and heating/cooling rate = 1 °C/min.

structure. In theoretical studies, Qi and Wang have suggested that the HPL structure has an ABAB... stacking sequence by means of a theory based on anisotropic composition fluctuations in the weak segregation limit.¹⁵

Thus, the stacking sequence of HPL structure has not been satisfactorily understood until now. In an effort to identify the stacking sequence of HPL, we have investigated the shear-induced HPL structure of the styrene–isoprene diblock copolymer through synchrotron SAXS.

Styrene–isoprene diblock copolymer (PSI67) was synthesized by living anionic polymerization using high vacuum techniques. The molecular weight of this sample measured with light scattering was 34 000, and the polydispersity index by GPC was 1.02. The weight fraction of polystyrene was 0.70 by ¹H NMR. The volume

* E-mail: wczin@postech.ac.kr. Tel.: +82-562-279-2136. Fax: +82-562-279-2399.

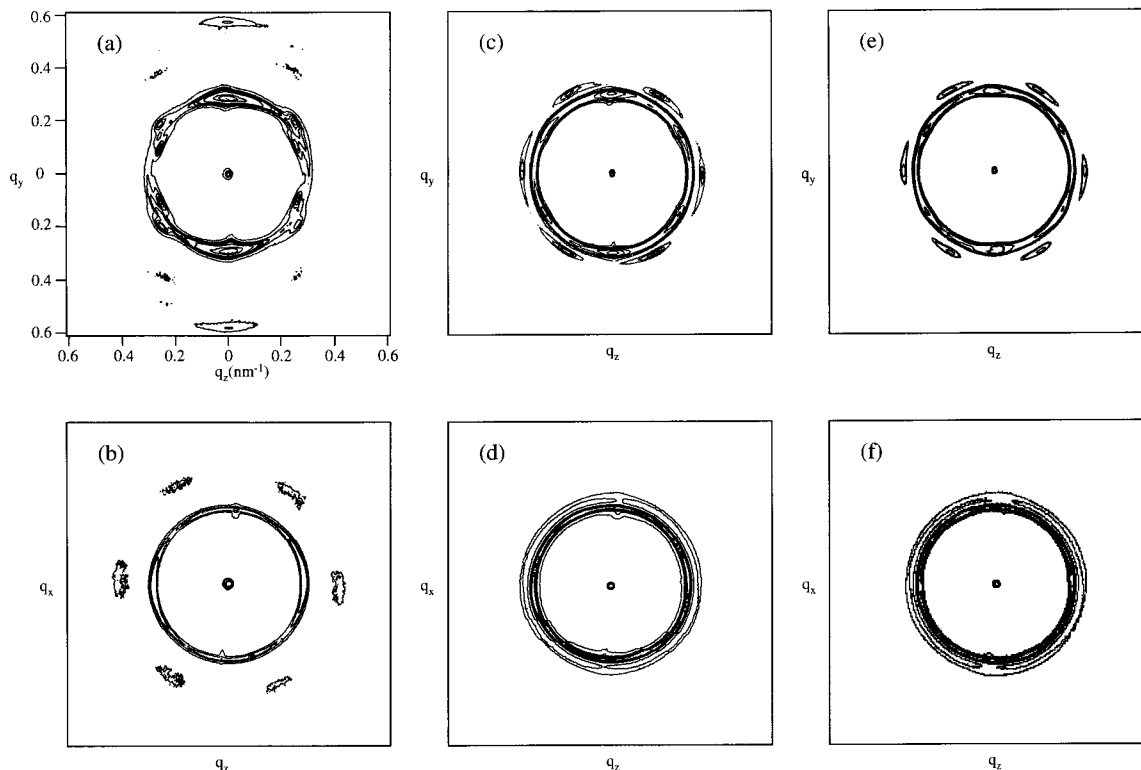


Figure 3. Contour plots of SAXS patterns for PSI67 in two directions: (a) and (b) obtained at 140 °C from the shear-oriented HPL structure, (c) and (d) taken at 180 °C after heating the samples, and (e) and (f) after cooling from 180 °C to 140 °C.

fraction of polystyrene was 0.67 when calculated with the densities 1.05 and 0.90 g/cm³ for polystyrene and polyisoprene, respectively. Samples were prepared by first dissolving a predetermined amount of PSI67 (10 wt %) in toluene in the presence of an antioxidant (Irganox 1010, Ciba-Geigy Group) and then slowly evaporating the solvent. After complete removal of the solvent, the samples were annealed at 120 °C for 24 h.

By using an advanced rheometric expansion system (ARES) with parallel plates of 25 mm in diameter, dynamic temperature sweep experiments were performed under a nitrogen environment with temperatures decreasing or increasing at a rate of 1 °C/min. The frequency (ω) of 0.1 rad/s and the strain amplitude (γ_0) of 1% were applied to the sample during heating and cooling.

Samples were aligned by using a large amplitude oscillatory shear. A frequency of 0.1 rad/s with 100% strain amplitude was applied at 140 °C for 1 h. This process was efficient to remove the grain boundary between microdomains in the samples. SAXS measurements were performed with point focusing (0.2 × 0.2 mm) at 1B2 beamline using synchrotron X-ray radiation sources at Pohang Accelerator Laboratory, Korea. The wavelength of X-ray source was 1.377 Å. Two-dimensional (2-D) diffraction patterns were recorded on imaging plates and read out with scanner (MAC Science). The distance between sample and imaging plate was 1.2 m. We designate x as the flow direction, y as the velocity gradient direction, and z as the vorticity direction. SAXS patterns were obtained with the X-ray beam directed along the x and y axes.

Phase-transition temperature of block copolymer can be identified by rheological measurements of the quantities such as the dynamic elastic shear (G') and loss moduli (G''). Here, we have conducted isochronal temperature scans to monitor changes in G' , which guide

the selection of temperatures for SAXS experiments. Figure 2 shows elastic modulus (G') for PSI67. G' continuously decreases as the temperature increases to 160 °C, at which temperature it starts to increase suddenly, indicating a phase transition between the two differently ordered states. On cooling, the transition does not take place. G' stays at a high value of the latter phase. It is noted that the low-temperature phase is not thermodynamically stable but the metastable phase is.

To identify each symmetry of phase detected in the dynamic shear moduli measurement, SAXS experiments were conducted on shear-aligned samples at 140 and 180 °C. The SAXS pattern at 140 °C, shown in Figure 3a, indicates a single-crystal-like orientation of the sample. The strong meridional reflections at ratios of 1:2 relative to the position of the first-order maximum (q^*) in the q_y - q_z plane reveal that layer planes are aligned in parallel with the shear planes. The two sets of off-meridional reflections in the inner and outer lowest reflections, whose locations are $68 \pm 1^\circ$ and $53 \pm 1^\circ$ with respect to the meridian, respectively, characterize the stacking of in-layer perforations. When combined with the results of rheology experiments, this pattern identifies the packing structure as HPL. The locations of the split, off-meridional reflections are different from those of HPL observed previously by Vigild et al.¹⁴ This implies that the HPL may have stacking sequences different from the model suggested by Vigild et al.

Figure 3b represents the diffraction pattern in the q_x - q_z plane. A weak isotropic diffraction ring is observed in the image. We believe that it is due to an imperfect alignment of the sample. As compared with Bragg peaks on the q_y - q_z plane of Figure 3a, it is found that it corresponds to the first-order peak of the layer. The weak 6-fold spots are also visible in the outer diffraction ring. This indicates the hexagonal in-plane symmetry

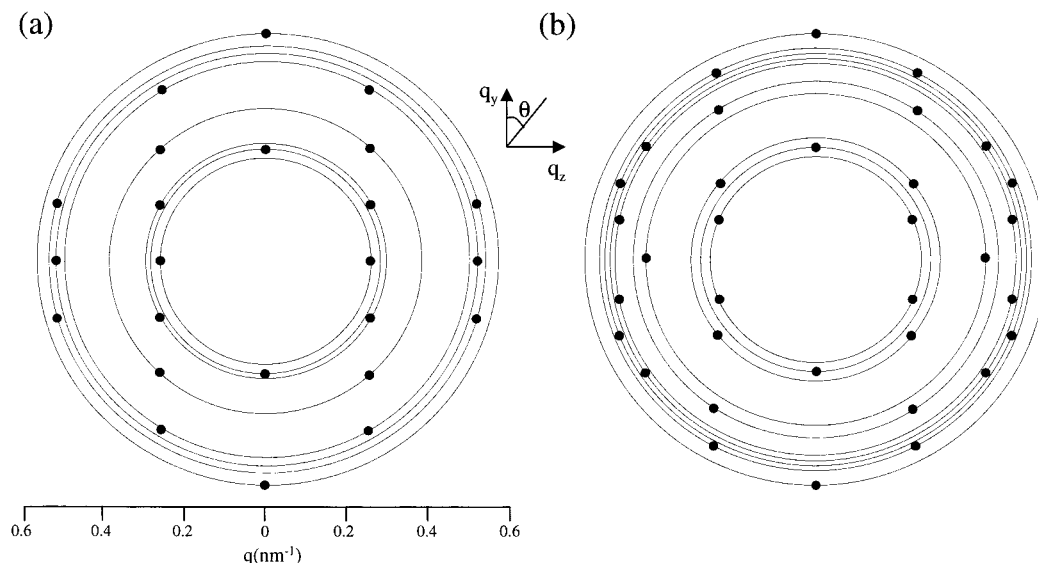


Figure 4. Positions of Bragg spots expected for hexagonal lattices of (a) ABAB... stacking (the lattice parameters, $a = 28$ and $c = 44$ nm) and (b) ABCABC... stacking ($a = 30$ nm and $c = 66$ nm). The hexagonal lattice parameters were taken on the values corresponded well to experimental results.

Table 1. Comparison of Observed Peak Positions and Azimuthal Angles of Spots with Those Predicted for ABAB... and ABCABC... Stackings

ABAB...stacking ^{a)}			ABCABC... stacking ^{b)}			observed	
relative peak position	azimuthal angle ($\pm\theta$) ^c	(hkl) ^d	relative peak position	azimuthal angle ($\pm\theta$)	(hkl)	relative peak position	azimuthal angle ($\pm\theta$)
1.00	90.0	(100)	1.00	68.3	(101)	1.00	67.7
1.09	0.0	(002)	1.09	0.0	(003)	1.10	0.0
1.14	61.3	(101)					
1.48	42.3	(102)	1.18	51.7	(102)	1.17	52.5
1.73	90.0	(110)	1.61	90.0	(110)		
1.92	30.7	(103)	1.73	32.9	(104)	1.73	31.2
			1.90	79.1	(201)		
			1.95	55.9	(113)		
2.00	90.0	(200)	2.00	68.9	(202)		
2.05	57.3	(112)	2.05	27.1	(105)	2.05	27.0
2.07	74.9	(201)					
2.18	0.0	(004)	2.18	0.0	(006)	2.19	0.0

^a Calculated by the lattice parameters: $a = 28$ and $c = 44$ nm. ^b Calculated by the lattice parameters: $a = 30$ and $c = 66$ nm. ^c Relative to the meridian (in degrees). ^d (hkl) are the indices in the three indices notation.

of the perforations in the layer.

Heating the sample to 180 °C produces the scattering patterns corresponding to those of the G phase.⁷ Figure 3c,d shows the contour plots of SAXS pattern at this temperature. Two sets of Bragg peaks with 6-fold symmetry are observed in the ratio of $(6)^{1/2}:(8)^{1/2}$ (Figure 3c). The lowest order reflections correspond to the family of first-order $\{211\}$ reflections in the G phase. Two of them are on the same parallel line as the strong meridional peaks from the layers in the HPL structure. This result confirms the previous findings^{8,14} for an epitaxial relationship between $\{211\}$ planes of G phase and the layer of HPL. Higher order reflections are also seen in the scattering pattern. In the q_y - q_z plane, $\{220\}$ diffraction peaks are located at $\pm 30^\circ$ relative to the first-order $\{211\}$ reflections. These two sets of six-spot pattern duplicates the previous SANS data obtained when the G phase has been grown from the shear-aligned hexagonally packed cylinders phase.⁷

Figure 3e,f shows the SAXS patterns obtained after cooling from 180 to 140 °C. These SAXS patterns indicate only the reflections characteristic of the G phase in Figure 3c,d without showing the indication of a partial transformation to the HPL structure. This

indicates that the HPL structure is an unusually long-lived nonequilibrium structure. This result is consistent with that observed in rheological measurements of Figure 2.

HPL signifies some possible sequences, i.e., ABAB..., ABCABC..., the combination of the two, and so on.^{8,11,15} Therefore, the stacking of HPL can be explained through the two hexagonal lattices for ABAB... and ABCABC... stacking as shown in Figure 1. Consideration of the periodicity and the symmetry of these stacking sequences leads us to calculate the position in scattering patterns. Figure 4 shows the calculated 2-D patterns of these two sequences for X-ray beam incident along the shear direction. When these are compared with the image of Figure 3a, within the limits of experimental accuracy, good correspondence is observed between the experimentally measured pattern and that calculated for ABCABC... stacking; in terms of interplanar angles and positions, all of the Bragg spots observed in Figure 3a can be explained with Figure 4b, whereas Figure 4a is not incapable of accounting for the positions of the four groups of off-meridional reflections, as shown in Table 1. This means that the perforations of HPL structure are stacked in the ABCABC... pattern.

In summary, this study found that the HPL structure is metastable and that the oriented HPL transforms into the G phase with six-spot patterns, confirming the previous report for the epitaxial relationship between the layer of HPL and {211} of G phases.^{8,14} Our scattering experiment on HPL structure led us to conclude that the perforations are stacked in the AB-CABC... pattern.

Acknowledgment. This work was supported by the Center for Advanced Functional Polymers (97K3-0206-03-02-3) and the Korea Research Foundation(1998-017-E00211). The SAXS measurements were performed at the Pohang Accelerator Laboratory (Beamline 1B2). We acknowledge Mr. Q.-J. Gu at POSTECH for kindly supplying the PSI samples.

References and Notes

- (1) Leibler, L. *Macromolecules* **1980**, *13*, 1602.
- (2) Hamley, I. W.; Koppi, K. A.; Rosedale, J. H.; Bates, F. S.; Almadal, K.; Mortensen, K. *Macromolecules* **1993**, *26*, 5959.
- (3) Disko, M. M.; Liang, K. S.; Behal, S. K.; Roe, R. J.; Jeon, K. J. *Macromolecules* **1993**, *26*, 2783.
- (4) Spontak, R. J.; Smith, S. D.; Ashraf, A. *Macromolecules* **1993**, *26*, 956.
- (5) Laurer, J. H.; Fung, J. C.; Sedat, J. W.; Agard, D. A.; Smith, S. D.; Samseth, J.; Mortensen, K.; Spontak, R. J. *Langmuir* **1997**, *13*, 2177.
- (6) Hajduk, D. A.; Harper, P. E.; Gruner, S. M.; Kim, C. C.; Thomas, E. L.; Fetters, L. J. *Macromolecules* **1994**, *27*, 4063.
- (7) Shulz, M. F.; Bates, F. S.; Almadal, K.; Mortensen, K. *Phys. Rev. Lett.* **1994**, *73*, 86.
- (8) Förster, S.; Khandpur, A. K.; Zhao, J.; Bates, F. S.; Hamley, I. W.; Ryan, A. J.; Bras, W. *Macromolecules* **1994**, *27*, 6922.
- (9) Khandpur, A. K.; Förster, S.; Bates, F. S.; Zhao, J.; Ryan, A. J.; Bras, W.; Hamley, I. W. *Macromolecules* **1995**, *28*, 8796.
- (10) Zhao, J.; Majumdar, B.; Shulz, M. F.; Bates, F. S.; Almadal, K.; Mortensen, K.; Hajduk, D. A.; Gruner, S. M. *Macromolecules* **1996**, *29*, 1204.
- (11) Shulz, M. F.; Khandpur, A. K.; Bates, F. S.; Almadal, K.; Mortensen, K.; Hajduk, D. A.; Gruner, S. M. *Macromolecules* **1996**, *29*, 2857.
- (12) Avgeropoulos, A.; Dair, B. J.; Hadjichristidis, N.; Thomas, E. L. *Macromolecules* **1997**, *30*, 5634.
- (13) Burger, C.; Micha, M. A.; Oesterich, S.; Förster, S.; Antonietti, M. *Europhys. Lett.* **1998**, *42*, 425.
- (14) Vigild, M. E.; Almdal, K.; Mortensen, K.; Hamley, I. W.; Faiclough, J. P. A.; Ryan, A. J. *Macromolecules* **1998**, *31*, 5702.
- (15) Qi, S.; Wang, Z.-G. *Macromolecules* **1997**, *30*, 4491.
- (16) Matsen, M. W.; Schick, M. *Phys. Rev. Lett.* **1994**, *72*, 2660.
- (17) Laradji, M.; Shi A.-C.; Noolandi, J.; Desai, R. C. *Macromolecules* **1997**, *30*, 3242.
- (18) Olmsted, P. D.; Miler, S. T. *Macromolecules* **1998**, *31*, 4011.

MA9912812